

# Processive RNA decay by the exosome

## Merits of a quantitative Bayesian sampling approach

Theresa Niederberger,<sup>1</sup> Sophia Hartung,<sup>2</sup> Karl-Peter Hopfner<sup>1,\*</sup> and Achim Tresch<sup>1,\*</sup>

<sup>1</sup>Department of Biochemistry, Center for Integrated Protein Sciences and Munich Center for Advanced Photonics at the Gene Center; Ludwig-Maximilians-University Munich; Munich, Germany; <sup>2</sup>Lawrence Berkeley National Lab; Berkeley, CA USA

**R**NA exosomes are large multi-subunit protein complexes involved in controlled and processive 3' to 5' RNA degradation. Exosomes form large molecular chambers and harbor multiple nuclease sites as well as RNA binding regions. This makes a quantitative kinetic analysis of RNA degradation with reliable parameter and error estimates challenging. For instance, recent quantitative biochemical assays revealed that degradation speed and efficiency depend on various factors, such as the type of RNA binding caps and the RNA length. We propose the combination of a differential equation model with Bayesian Markov Chain Monte Carlo (MCMC) sampling for a more robust and reliable analysis of such complex kinetic systems. Using the exosome as a paradigm, it is shown that conventional "best fit" approaches to parameter estimation are outperformed by the MCMC method. The parameter distribution returned by MCMC sampling allows for a reliable and meaningful comparison of the data from different time series. In the case of the exosome, we find that the cap structures of the exosome have a direct effect on the recruitment and degradation of RNA, and that these effects are RNA length-dependent. The described approach can be widely applied to any processive reaction with a similar kinetics like the XRN1-dependent RNA degradation, RNA/DNA synthesis by polymerases and protein synthesis by the ribosome.

### Introduction

The turnover, processing and quality control of cellular RNAs are executed by a variety of endo/exonucleases. For instance, RNA decay is performed either by 5'-3' exonucleases, such as XRN1 (*H. sapiens*)/pacman (*D. melanogaster*)/KEM1 (*S. cerevisiae*) or by 3'-5' exonucleases like the archaeal/eukaryotic exosome or the prokaryotic degradosome.<sup>1,2</sup> In both cases the RNA molecule is degraded sequentially, in a one-by-one nucleolytic manner, often after a preceding and priming endonucleolytic cut. Degradation is highly regulated and its efficiency depends on various factors such as the structure of the nuclease and the primary and secondary structure of the substrate. While research over the past years established the core structure and biochemical mechanism as well as provided a first inventory of a multitude of regulatory factors,<sup>3-5</sup> a quantitative analysis of these machineries in terms of substrate specificities and preferences was difficult to conduct because of the inherent complexity of the involved kinetics. Yet the comparison of degradation kinetics of different enzyme mutants or substrates can provide valuable information on functionally relevant architectural features of the exosome and other processive machineries. A variety of research groups have obtained a wealth of data from time series measurements of RNA decay profiles of the exosome on gels with single nucleotide resolution.<sup>6-10</sup> In principle, these data should allow to extract defined kinetic parameters

**Key words:** RNA degradation, exosome structure, processive enzymes, enzyme kinetics, bayesian inference, parameter estimation, Markov Chain Monte Carlo sampling

Submitted: 08/03/10

Revised: 10/28/10

Accepted: 10/31/10

DOI: 10.4161/rna.8.1.14067

\*Correspondence to: Karl-Peter Hopfner and Achim Tresch;  
Email: hopfner@lmb.uni-muenchen.de and tresch@lmb.uni-muenchen.de

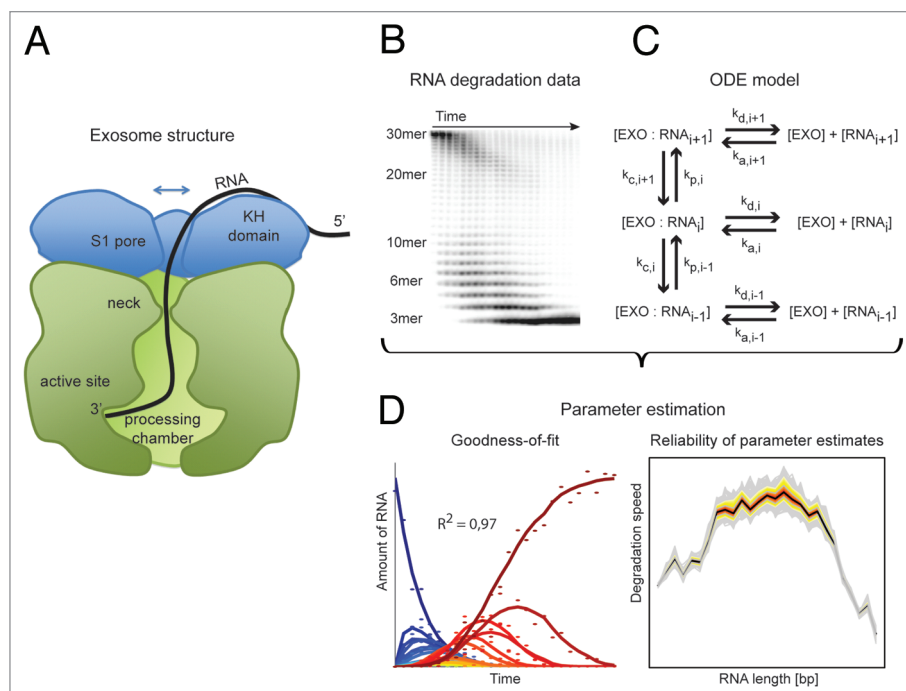


**Figure 1.** Exosome structure, experiment design and analysis. (A) Sketch of the exosome consisting of a cap structure (blue) and a ring structure (green), with RNA inserted to it (black strand). The ring contains a constriction (the neck region) in its upper part, and three catalytic sites in its lower part. The distance from the RNA 3' end at the catalytic site to the neck region is approx. 15 nt. (B) Data showing an RNA degradation time series. Each column of the gel corresponds to one time point, and each row corresponds to an RNA population of a certain length  $i = 3, \dots, 30$ . (C) System of ordinary differential equations (ODEs) describing the degradation of each RNA population in a separate reaction step. Four types of reactions or the kinetic parameters that determine the dynamics of the system: association ( $k_{a,i}$ ), dissociation ( $k_{d,i}$ ), cleavage ( $k_{c,i}$ ) and polymerization ( $k_{p,i}$ ). (D) Sample result of the parameter estimation for the ODE model in (C) with the data shown in (B). The left hand side plot assesses the quality of a given parameter set. The data are displayed as dots, one color for each RNA length, from 30mers (blue) to 3mers (red). The curves represent the fit, colored correspondingly. The goodness-of-fit measure is reported as 0.97, this is a good fit. The right hand side plot assesses the variance in parameter estimation; one parameter for each RNA length is shown. The colored bands indicate the variation in the parameter estimates (see Fig. 2).

for degradation of intermediates. Only recently, a quantitative modeling based on ordinary differential equations has been established.<sup>11</sup> Using Bayesian statistics in combination with an elaborate Monte Carlo sampling technique, not only kinetic parameter estimates can be derived, but—equally important—insight is gained into parameter uncertainty and their dependency from the experimental data.<sup>12</sup> The purpose of this article is to highlight the importance and merits of an accurate and thorough mathematical modeling for the interpretation of biological processes. The exosomal degradation of RNA molecules serves to illustrate the advantages of a Bayesian sampling approach as a versatile tool for this purpose.

### The Exosome is a Processive RNA-Degrading Enzyme

Degradation and processing of 3'→5' RNA are in large part performed by the

eukaryotic and archaeal RNA exosome or bacterial exosome-like complexes, which are involved in rRNA maturation, non-coding and mRNA decay and RNA quality control.<sup>13</sup> Quite remarkably, the mode of RNA degradation by exosomes has changed through evolution: in archaea and bacteria, the core exosome subunits are active and possess phosphate dependent nuclease as well as nucleoside diphosphate dependent polymerization activity. In contrast, while eukaryotic exosomes retained all subunits and the overall structure of the active archaeal exosome core, they lost phosphorolytic nuclease/polymerization activities and instead acquired additional hydrolytic nucleases and interact with poly-adenylases.<sup>14</sup> Still the composition and structural architecture of the exosome complex is astonishingly conserved through all kingdoms of life. All exosomes have a barrel like structure with a central protected chamber and RNA binding proteins forming the top surface.

In the archaeal exosome, which was used in the highlighted study, three active sites are located in this chamber.<sup>15</sup> Based on a variety of experimental evidence,<sup>7,8,16</sup> single-stranded (ss)RNA is proposed to bind to the RNA binding proteins on top of the complex, threaded through a narrow neck into the chamber and degraded (Fig. 1A). On the basis of these findings, a homopolymeric 30mer ssRNA molecule can be used to compare the degradation characteristics of a wild-type archaeal exosome with single-site mutants and complex variants containing different RNA binding proteins. The product of one step of the exosomal RNA decay is at the same time the substrate for the next step, or alternatively can dissociate and bind to another complex for further degradation. Experimentally, such a processive degradation can be well captured by time series measurements on a high resolution sequencing gel, where the columns on the gel correspond to time points, and

the rows correspond to different lengths of the processed molecule (Fig. 1B). The time dependent changes in the amounts of RNA degradation intermediates of different lengths can be appropriately modeled by a set of ordinary differential equations (ODEs).<sup>17</sup> The processed molecule (the RNA) needs to be bound to the degrading enzyme (the exosome), thus the basic model of RNA decay is formed by four reactions: association of RNA to the exosome, dissociation of RNA from the exosome, degradation of bound RNA and polymerization of bound RNA (Fig. 1C). The reaction rates in this ODE model are the parameters to be determined from noise-containing data, a problem which is called a regression problem in statistics, or an inverse problem in physics. Typically, such a problem is *ill-posed*, i.e., a solution does not necessarily exist, and if one exists, it does not have to be unique, and it may vary unstably in response to small changes in the measurements.<sup>18</sup> A sound parameter estimation procedure therefore needs to address all these issues by not only producing one single parameter fit, but by providing information about the goodness of this fit and the variability of the estimation process (Fig. 1D).

### Model Selection is Crucial for Successful Parameter Estimation

To alleviate the problem of ill-posedness, a candidate model needs to be flexible enough to contain a solution which explains the data sufficiently well. Standard optimization procedures can be used to search for a parameter set which, if plugged into the model, should reproduce the observed data up to some acceptable error. The latter is usually measured by the goodness-of-fit ( $R^2$ -value, see Fig. 1D).<sup>19</sup> If several models are capable of explaining the data, the one containing the fewest parameters is preferable. This common sense but nevertheless important principle is often referred to as Occam's razor.<sup>20</sup> In a reverse conclusion, the search for a good model implies the search for a minimal model. Moreover, the removal of redundant variables is a prerequisite for unambiguous solutions.

The straightforward model in the RNA degradation setting consists of 108 parameters: association ( $k_{a,i}$ ), dissociation

( $k_{d,i}$ ), cleavage ( $k_{c,i}$ ) and polymerization ( $k_{p,i}$ ) rates for every RNA molecule from length  $i = 30$  to length 4 (the amount of RNA of length 3 has only been measured as a final product, see Fig. 1B). It is easy to find good parameter solutions for this model (data not shown). Since the polymerization reaction can be neglected due to a large excess of inorganic phosphate over RNA or its ADP degradation products during the course of the experiment, the number of parameters can be reduced to 81 without affecting the goodness-of-fit. Note further that bound and free RNA cannot be measured individually, thus the remaining parameters are still redundant: Proportional scaling of association and cleavage rates leads to almost identical results (data not shown). A reparametrization in combination with a parameter reduction can cure these problems. This has been achieved by replacing association, dissociation and cleavage by the so-called *catalytic efficiency*  $e_i = k_{a,i} k_{c,i} / (k_{d,i} + k_{c,i})$ , a term similar to the Michaelis constant ( $K_M$ ) in Michaelis-Menten type kinetics. The remaining 28 parameters (27 length-specific catalytic efficiencies and one global cleavage rate) still suffice for a good approximation (Fig. 1D) and are identifiable. The next paragraph describes how Bayesian statistics may help to assess parameter identifiability and to eventually identify groups of redundant parameters.

### Bayesian Statistics and Monte Carlo Sampling Provide More than a Point Estimate of the Parameters

The standard frequentist approach to parameter identification is to find a parameter set  $\theta$  that maximizes a likelihood function  $L(\theta)$ , the *maximum likelihood* estimate.<sup>20</sup> Under the assumption of independent observations with Gaussian measurement errors, this function is the sum of the squared errors, and the resulting approach is well-known as least squares estimation. While the likelihood function is helpful to verify that the model can approximate the data, nothing can be said about the uniqueness of the solution or the variability of the parameter estimates as a function of the data (Fig. 2A). The Bayesian viewpoint to parameter

estimation does not consider the parameters  $\theta$  fixed, but as random variables that depend on the given data and that may vary according to our prior beliefs. In other words, starting with a pre-defined *prior* parameter distribution, the data is used to update our beliefs and arrive at a *posterior* parameter distribution which contains all information on the parameters that can be learned from the data.<sup>20</sup> In particular, one can answer questions like "Are the association and dissociation parameters for one RNA length dependent?" or "Is the parameter distribution of the catalytic efficiency narrow or wide?" in a precise way by calculating statistical measures of dependence or dispersion, respectively. If two posterior distributions from two different experiments are available, we can even compare models by asking, e.g., for the probability that the catalytic efficiency  $e_i$  in experiment 1 is higher than in experiment 2. In this setting, the analogue of the maximum likelihood estimate is the *maximum a posteriori* estimate, a parameter set which maximizes the posterior.

All this convenience comes at a cost. First, the prior distribution needs to be chosen with utmost care. An overly strong prior may override or bias any evidence from the data. A weak prior may result in an unnecessarily disperse posterior distribution. Since the effect of the prior choice cannot be assessed from the data, it is mandatory to perform simulations. In such a simulation scenario, a realistic, "true" parameter set is chosen; noise-containing measurements are simulated from it, and the posterior is calculated using the candidate prior. The quality of the posterior can then be quantified exactly, and a suitable prior can be selected. The second severe obstacle to Bayesian parameter estimation is that generally the posterior distribution cannot be derived analytically. This long-standing problem was brilliantly solved by Markov Chain Monte Carlo (MCMC) sampling,<sup>21-23</sup> one of the major breakthroughs in 20<sup>th</sup> century statistics. MCMC outputs a sequence (Markov chain) of parameter sets whose empirical distribution, for long sequences, approximates (converges to) the posterior distribution. Thus any question that one might ask about the posterior parameter distribution can, in theory, be answered by looking at a corresponding

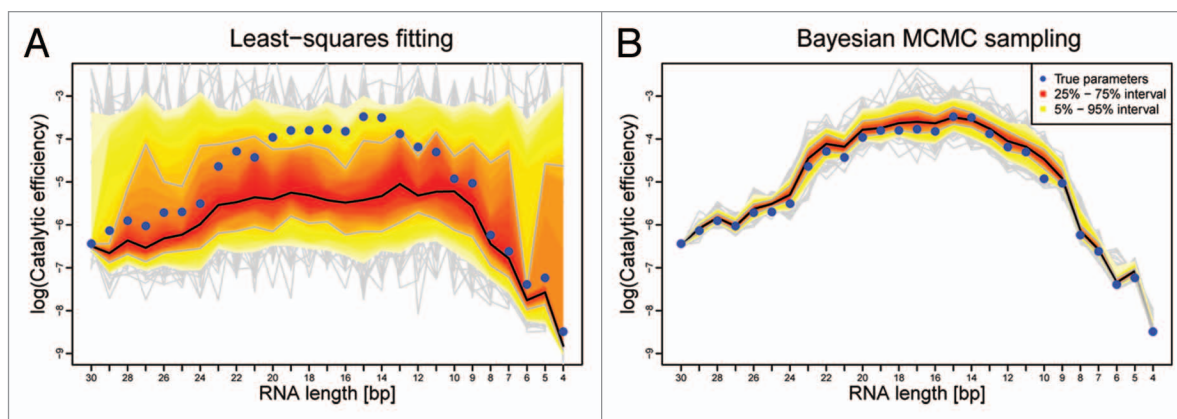


**Figure 2.** Simulation study comparing the parameter estimation quality for (A) least squares fitting and (B) Bayesian MCMC sampling. The blue points represent the “true” kinetic parameters that we fixed throughout the whole simulation. The RNA concentration time courses are obtained as the solution of the ODE model in Fig. 1C. Synthetic measurements were generated by adding independent Gaussian noise to all the log RNA concentrations in the time series. The maximum likelihood and the maximum a posteriori estimates were calculated as described in the main text, and this procedure was repeated 100 times. The results are visualized as a quantile profile plot: The red (yellow) band marks the central 95% (50%) intervals for the estimated catalytic efficiencies  $e_i$ , for  $i = 30, \dots, 4$  nt. (A) shows the central 95% (50%) intervals of the 100 least squares parameter estimates. (B) shows Bayesian confidence intervals, averaged over 100 runs. Bayesian sampling clearly exhibits less variance (narrower bands) and a smaller bias (bands are closer to the true parameters) than least squares fitting.

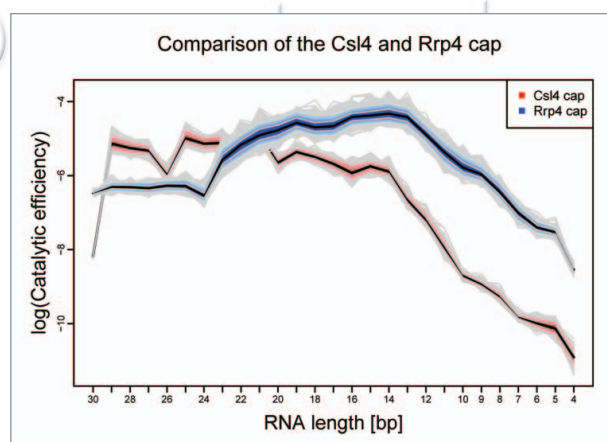


**Figure 3.** Comparison of the exosomes with Csl4 and Rrp4 cap structure. Catalytic efficiencies  $e_i$  of the Csl4 cap exosome (red) and the Rrp4 cap exosome (blue) are shown on the y-axis as a function of the RNA length from  $i = 30$  nt to 4 nt (x-axis). We generated 10 Markov chains of length  $2 \times 10^5$  and randomly sampled  $10^4$  parameter sets from the last  $10^5$  entries of these chains. The quantile profile plot shows the 50% Bayesian confidence intervals (dark color) and the 100% intervals (light color) of the sampled catalytic efficiencies. If the Rrp4 and the Csl4 bands do not overlap at some length  $i$ , this means that under the assumptions of the model, the catalytic efficiencies  $e_i$  of Rrp4 and Csl4 differ with an estimated probability of 99.99%.

Markov chain. Still, care must be taken to ensure that the Markov chain is long enough to have the desired properties, and this again needs to be checked in time-consuming simulations. The increased computational effort is rewarded with a solid, meaningful joint posterior distribution of the model parameters (Fig. 2B).

### Structural Variations in the Exosome Imply Functional Differences in RNA Processing

In the archaeal exosome experiment, we chose a Gaussian likelihood function. As for the prior, we did not want to impose any restrictions on the absolute values of

the parameters. Instead, we formalized the physically meaningful assumption that catalytic efficiencies should vary smoothly with the RNA length. Our prior therefore penalizes the sum of all absolute differences of two successive catalytic efficiencies. It contains only one free parameter which was tuned in simulations beforehand. We verified the rapid convergence (mixing) of the resulting Markov Chain (data not shown, reviewed in ref. 11). When Bayesian MCMC sampling was applied to the RNA degradation data to compare two exosome variants with Rrp4 or Csl4 cap structures, it revealed a clear difference between their degradation kinetics (Fig. 3). Note that the kinetics of RNA degradation can only be explained by a model that includes association and dissociation rate constants, i.e., the exosome is not strictly processive. It is important to point out that this is association and dissociation of the 3'-end of the RNA to the active site and not of the whole RNA molecule to the protein. Longer RNAs may just stay bound to the caps and the neck of the processing chamber while moving to and away from the active site. More can be said about the role of the cap proteins and their RNA binding sites: Rrp4 recruits the poly rA substrate more efficiently to the exosome than Csl4. The cap structures



surprisingly also differ in their efficiency to degrade small RNAs that are too short to be simultaneously in contact with the active site and the cap proteins (see Fig. 1A). From the crystal structures of both exosome variants we know that the Rrp4 protein more intimately interacts with the ring of the processing chamber than Csl4.<sup>3</sup> It is not unlikely that this can influence the flexibility of the core ring and hence the degradation dynamics.

Bayesian sampling was further used to elucidate the role of single amino acid side chains in the neck region and close to the active site.<sup>11</sup> An arginine in the neck region seems to be crucial for threading the RNA through the narrow neck into the processing chamber and a tyrosine close to the active site clearly stabilizes the 3'-end of the RNA. From comparing crosslinked exosome complexes with the wild-type this suggests that the ring architecture needs to breathe or display some conformational dynamics to increase the size of the neck. Only after the RNA molecule is bound in the neck the protein ring might tightly close around its substrate. A recent report furthermore established that the yeast exosome, despite of having lost its phosphorolytic RNase and polymerization active sites, still appears to channel RNA through the ring, to feed an ectopically bound hydrolytic nuclease (Rrp44).<sup>7</sup>

## Summary and Outlook

The interplay of quantitative biochemistry and innovative statistics may lead to a qualitative leap in the interpretation of experimental results. Once an appropriate model is found, Bayesian parameter inference in combination with MCMC generates a posterior parameter distribution from the data and from prior knowledge. Both prior choice and MCMC require extensive simulations to verify their correct operation. A huge benefit of the Bayesian approach is that the posterior parameter distribution can be used to assign probabilities to any hypothesis about the parameters or their relations. The application to the RNA degradation by the archaeal exosome proved that different cap structures have direct and indirect consequences on the catalytic efficiency, which might be explained by

association of RNA to the cap or by modification of the exosomal ring.

This points towards a future research direction, namely the recruitment and loading mechanisms of RNA substrates to the exosome. Given the functional association of 3' homopolymeric and heteropolymeric tails in exosome associated RNA metabolism, an investigation of ectopic sequence-specific RNA binding domains of the exosome on differently tailed (unstructured) RNA seems promising. Exosome mutants with destroyed or crosslinked ring structure show enhanced or reduced degradation of RNA,<sup>11</sup> which suggests that lateral opening of the exosome might be necessary for RNA recruitment. Therefore, it will be interesting to test loading factor activities e.g., for yeast SKI and TRAMP complexes, two key accessory factors for the degradation of cytoplasmic and nuclear RNAs.<sup>24,25</sup> In sum, a quantitative analysis can reveal a variety of features that are important for the catalytic efficiency of the exosome and might be used to gain a deeper understanding of substrate preference and degradation regulation.

Although the analysis described here has been tailored to the kinetics of the RNA degradation by the archaeal exosome, it is by no means limited to this system. Needless to say, the Bayesian sampling method is well suited to address the RNA degradation by the eukaryotic exosome, for instance to reveal the interplay between endo- and exonuclease activities<sup>26-28</sup> and biochemical differences between different Dis3/Dis3L isoforms as well as Rrp6 of the human exosome complex.<sup>29-31</sup> Related systems of interest are the degradation of 5' ends by XRN1, RNA degradation by bacterial degradosomes, or in general any system that involves the (semi)processive synthesis or degradation of biopolymers.

## Acknowledgements

This work was supported by grants from the German research council (Sonderforschungsbereich 646 and HO2489/3) and the German Excellence Initiative (Center for Integrated Protein Sciences and Munich Center for Advanced Photonics). A.T. was supported by an LMU<sup>excellent</sup> professorship to Patrick Cramer.

## References

- Mitchell P, Petfalski E, Shevchenko A, Mann M, Tollervey D. The exosome: a conserved eukaryotic RNA processing complex containing multiple 3'→5' exoribonucleases. *Cell* 1997; 91:457-66.
- Muhlrad D, Decker CJ, Parker R. Deadenylation of the unstable mRNA encoded by the yeast MFA2 gene leads to decapping followed by 5'→3' digestion of the transcript. *Genes Dev* 1994; 8:855-66.
- Büttner K, Wenig K, Hopfner KP. Structural framework for the mechanism of archaeal exosomes in RNA processing. *Mol Cell* 2005; 20:461-71.
- Liu Q, Greimann JC, Lima CD. Reconstitution, activities and structure of the eukaryotic RNA exosome. *Cell* 2006; 127:1223-37.
- Lorentzen E, Conti E. Structural basis of 3' end RNA recognition and exoribonucleolytic cleavage by an exosome RNase PH core. *Mol Cell* 2005; 20:473-81.
- Allmang C, Petfalski E, Podtelejnikov A, Mann M, Tollervey D, Mitchell P. The yeast exosome and human PM-Scl are related complexes of 3'→5' exonucleases. *Genes Dev* 1999; 13:2148-58.
- Bonneau F, Basquin J, Ebert J, Lorentzen E, Conti E. The yeast exosome functions as a macromolecular cage to channel RNA substrates for degradation. *Cell* 2009; 139:547-59.
- Navarro MV, Oliveira CC, Zanchin NI, Guimaraes BG. Insights into the mechanism of progressive RNA degradation by the archaeal exosome. *J Biol Chem* 2008; 283:14120-31.
- Oddone A, Lorentzen E, Basquin J, Gasch A, Rybin V, Conti E, et al. Structural and biochemical characterization of the yeast exosome component Rrp40. *EMBO Rep* 2007; 8:63-9.
- Portnoy V, Evguenieva-Hackenberg E, Klein F, Walter P, Lorentzen E, Klug G, et al. RNA polyadenylation in Archaea: not observed in *Haloferax* while the exosome polynucleotidylates RNA in *Sulfolobus*. *EMBO Rep* 2005; 6:1188-93.
- Hartung S, Niederberger T, Hartung M, Tresch A, Hopfner KP. Quantitative analysis of processive RNA degradation by the archaeal RNA exosome. *Nucleic Acids Res* 2010; 38:5166-76.
- Bolstad WM. Understanding Computational Bayesian Statistics. John Wiley 2010.
- Houssley J, LaCava J, Tollervey D. RNA-quality control by the exosome. *Nat Rev Mol Cell Biol* 2006; 7:529-39.
- Hartung S, Hopfner KP. Lessons from structural and biochemical studies on the archaeal exosome. *Biochem Soc Trans* 2009; 37:83-7.
- Walter P, Klein F, Lorentzen E, Ilchmann A, Klug G, Evguenieva-Hackenberg E. Characterization of native and reconstituted exosome complexes from the hyperthermophilic archaeon *Sulfolobus solfataricus*. *Mol Microbiol* 2006; 62:1076-89.
- Lorentzen E, Dziembowski A, Lindner D, Seraphin B, Conti E. RNA channelling by the archaeal exosome. *EMBO Rep* 2007; 8:470-6.
- Klipp E, Liebermeister W, Wierling C, Kowald A, Leirach H, Herwig R. Systems Biology: A Textbook. Wiley-VCH 2009.
- Hadamard J. Sur les problèmes aux dérivées partielles et leur signification physique. Princeton University Bulletin 1902; 49-52.
- Barlow RJ. Statistics: A Guide to the Use of Statistical Methods in the Physical Sciences (Manchester Physics Series). Wiley 1989.
- MacKay D. Information theory, inference and learning algorithms. Cambridge University Press 2007.
- Hastings WK. Monte Carlo sampling methods using Markov chains and their Applications. *Biometrika* 1970; 57:97-109.
- Andrieu C, de Freitas N, Doucet A, Jordan M. An Introduction to MCMC for Machine Learning. Machine Learning 2003; 50:5-43.

23. Gilks WR, Richardson S, Spiegelhalter DJ. Markov Chain Monte Carlo in Practice. Chapman and Hall/CRC 1995.
24. Anderson JS, Parker RP. The 3' to 5' degradation of yeast mRNAs is a general mechanism for mRNA turnover that requires the SKI2 DEVH box protein and 3' to 5' exonucleases of the exosome complex. EMBO J 1998; 17:1497-506.
25. LaCava J, Houseley J, Saveanu C, Petfalski E, Thompson E, Jacquier A, et al. RNA degradation by the exosome is promoted by a nuclear polyadenylation complex. Cell 2005; 121:713-24.
26. Lebreton A, Tomecki R, Dziembowski A, Seraphin B. Endonucleolytic RNA cleavage by a eukaryotic exosome. Nature 2008; 456:993-6.
27. Schaeffer D, Tsanova B, Barbas A, Reis FP, Dastidar EG, Sanchez-Rotunno M, et al. The exosome contains domains with specific endoribonuclease, exoribonuclease and cytoplasmic mRNA decay activities. Nat Struct Mol Biol 2009; 16:56-62.
28. Schneider C, Leung E, Brown J, Tollervey D. The N-terminal PIN domain of the exosome subunit Rrp44 harbors endonuclease activity and tethers Rrp44 to the yeast core exosome. Nucleic Acids Res 2009; 37:1127-40.
29. Staals RH, Bronkhorst AW, Schilders G, Slomovic S, Schuster G, Heck AJ, et al. Dis3-like 1: a novel exoribonuclease associated with the human exosome. EMBO J 2010; 29:2358-67.
30. Midtgaard SF, Assenolt J, Jonstrup AT, Van LB, Jensen TH, Brodersen DE. Structure of the nuclear exosome component Rrp6p reveals an interplay between the active site and the HRDC domain. Proc Natl Acad Sci USA 2006; 103:11898-903.
31. Tomecki R, Kristiansen MS, Lykke-Andersen S, Chlebowski A, Larsen KM, Szczesny RJ, et al. The human core exosome interacts with differentially localized processive RNases: hDIS3 and hDIS3L. EMBO J 29:2342-57.

©2011 Landes Bioscience.  
Do not distribute.